
DIRECT: Deep Active Learning under Imbalance and Label Noise

Shyam Nuggehalli^{*1} Jifan Zhang^{*1} Lalit Jain² Robert Nowak¹

Abstract

Class imbalance is a prevalent issue in real world machine learning applications, often leading to poor performance in rare and minority classes. With an abundance of wild unlabeled data, active learning is perhaps the most effective technique in solving the problem at its root – collecting a more balanced and informative set of labeled examples during annotation. Label noise is another common issue in data annotation jobs, which is especially challenging for active learning methods. In this work, we conduct the first study of active learning under both class imbalance and label noise. We propose a novel algorithm that robustly identifies the class separation threshold and annotates the most uncertain examples that are closest from it. Through a novel reduction to one-dimensional active learning, our algorithm DIRECT is able to leverage the classic active learning literature to address issues such as batch labeling and tolerance towards label noise. We present extensive experiments on imbalanced datasets with and without label noise. Our results demonstrate that DIRECT can save more than 60% of the annotation budget compared to state-of-art active learning algorithms and more than 80% of annotation budget compared to random sampling.

1. Introduction

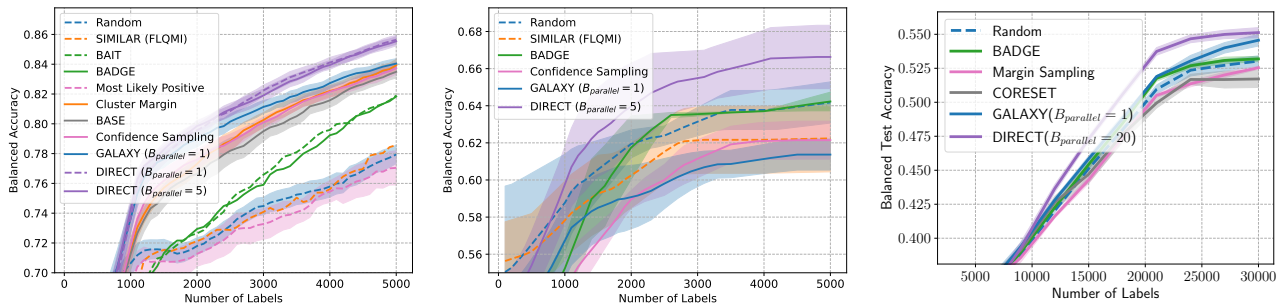
Large-scale deep learning models are playing increasingly important roles across many industries. Human feedback and annotations have played a significant role in developing such systems through. Progressively over time, we believe the role of humans in a machine learning pipeline would shift to annotating rare yet important cases. However, under data imbalance, the typical strategy of randomly choosing examples for annotation becomes especially inefficient.

^{*}Equal contribution ¹University of Wisconsin-Madison
²Michael G. Foster School of Business, University of Washington.
 Correspondence to: Jifan Zhang <jifan@cs.wisc.edu>.

This is because the majority of the labeling budget would be spent on common and well-learned classes, resulting in insufficient rare class examples for training an effective model. For many annotation jobs, this challenge of data imbalance is further compounded by label noises induced from annotators. In this paper, we mitigate these issues by proposing a deep active learning strategy. Our algorithm DIRECT sequentially and adaptively chooses informative and more class-balanced examples for annotation while being robust to noisy annotations. To the best of our knowledge, this is the first deep active learning study to address the challenging yet prevalent scenario where both imbalance and label noise coexist.

Inspired by previous work by Zhang et al. (2022), we propose a novel reduction of the imbalanced classification problem into one-dimensional active learning problems. For each class, our reduction sorts unlabeled examples into an list ordered by one-vs-rest margin scores. The goal of DIRECT is to find the *optimal separation threshold* which best separates the examples in any given class from the rests. With an equivalence to finding the best threshold classifier, we were able to employ classic active learning literature for obtaining the separation threshold. Once the optimal separation threshold is identified, DIRECT annotates a set of more class-balanced examples near this threshold. As examples around the optimal separation threshold tend to have high uncertainty, DIRECT annotates examples that are both class-balanced and informative.

With the reduction to classic one-dimensional active learning literature, DIRECT also inherits the advantages from classic active learning algorithms such as robustness against label noise and batch labeling. This is in contrast to the state-of-art imbalanced active learning algorithm GALAXY proposed by Zhang et al. (2022), which requires sequential labeling and is much less robust against label noise. As demonstrated in Figure 1, under both noisy and noiseless label settings, DIRECT improves significantly over GALAXY’s label efficiency – DIRECT requires less annotations to achieve the same accuracy. It achieves state-of-art label efficiency gain on both supervised fine-tuning of ResNet-18 and semi-supervised fine-tuning of large pre-trained model under the LabelBench framework (Zhang et al., 2023a). Lastly, DIRECT also allows for parallel annotations with various batch sizes.



(a) Imbalanced CIFAR-10, two classes, no label noise. (b) Imbalanced CIFAR-100, two classes, 20% label noise. (c) LabelBench FMoW (62 classes with imbalance), no label noise

Figure 1: Performance of DIRECT over existing baselines for both noiseless and noisy settings. The x-axis represents the total number of labeled examples so far and the y-axis shows the neural network’s balanced accuracy. Both (a) and (b) are using supervised training of ResNet-18. In (c), we finetune CLIP ViT-B32 model in combination of semi-supervised training under the LabelBench framework (Zhang et al., 2023a). B_{parallel} is the batch size indicating the number of parallel annotators for the annotation job. $B_{\text{parallel}} = 1$ indicates the synchronous annotation requirement by GALAXY. Our algorithm DIRECT takes pre-specified B_{parallel} as input, which is determined by real world decisions.

To summarize our main contributions:

- We propose a novel reduction that bridges the advancement in theoretical active learning literature to imbalanced active classification for deep neural networks.
- Our algorithm DIRECT addresses the prevalent imbalance and label noise issues and annotates a more class-balanced and informative set of examples.
- Compared to state-of-art algorithm GALAXY (Zhang et al., 2022), DIRECT allows parallel annotation by multiple annotators while still maintaining significant label-efficiency improvement.
- We conduct experiments across eight dataset settings, four levels of label noise and for both ResNet-18 and large pretrained model (CLIP ViT-B32). DIRECT consistently performs the best compared against existing baseline algorithms. Quantitatively, DIRECT can save more than 60% annotation cost compared to GALAXY, and more than 80% annotation cost compared to random sampling.

2. Related Work

Class-Balanced Deep Active Learning Active Learning strategies sequentially and adaptively choose examples for annotation (Settles, 2009). Many uncertainty-based deep active learning methods extend the traditional active learning literature such as margin, least confidence and entropy sampling (Tong & Koller, 2001; Settles, 2009; Balcan et al., 2006; Kremer et al., 2014). These methods have also been shown to perform among top methods when fine-tuning large pretrained models and combined with semi-supervised learning algorithms (Zhang et al., 2023a). More sophisticated methods have also been proposed to optimize the

chosen unlabeled examples’ uncertainty (Gal et al., 2017; Ducoffe & Precioso, 2018; Beluch et al., 2018), diversity (Sener & Savarese, 2017; Geifman & El-Yaniv, 2017; Citovsky et al., 2021), or a mix of both (Ash et al., 2019; 2021; Wang et al., 2021; Elenter et al., 2022; Mohamadi et al., 2022). However, these methods often perform poorly under prevalent and realistic scenarios such as under label noises (Khosla et al., 2022) or under class imbalance (Kothawade et al., 2021; Zhang et al., 2022; 2023a).

Deep Active Learning under Imbalance Data imbalance and rare instances are prevalent in almost all modern machine learning applications. Active learning techniques are effective in addressing the problem in its root by collecting a more class-balanced dataset (Aggarwal et al., 2020; Kothawade et al., 2021; Emam et al., 2021; Zhang et al., 2022; Coleman et al., 2022; Jin et al., 2022; Cai, 2022; Zhang et al., 2023b). To this end, Kothawade et al. (2021) propose a submodular-based method that actively annotates examples similar to known examples of rare instances. Our work is motivated by Zhang et al. (2022), where they propose GALAXY, an algorithm that construct one-dimensional linear graphs and apply graph-based active learning techniques in annotating a set of examples that are both class-balanced and uncertain. While GALAXY outperforms existing algorithms, due to a bisection procedure involved, it does not allow parallel annotation. In addition, bisection procedures are generally not robust against label noises, a prevalent challenge in real world annotation tasks. Our algorithm DIRECT mitigates all of the above shortcomings of GALAXY while outperforming it even with synchronous labeling and no label noise, beating GALAXY in its own game.

Lastly, we distinguish our work from Zhang et al. (2023b), where the paper studies the algorithm selection problem. Unlike our goal of proposing a new deep active learning algorithm, the paper proposes meta algorithms to choose the right active learning algorithm among a large number of candidate algorithms.

Deep Active Learning under Label Noise Label noisy settings has rarely been studied in the deep active learning literature. Related but tangential to our work, several papers have studied to use active learning for cleaning existing noisy labels (Lin et al., 2016; Younesian et al., 2021). In this line of work, they assume access to an oracle annotator that will provide clean labels when queried upon. This is fundamentally different from our work, where our annotator may provide noisy labels. Another line of more theoretical active learning research studies active learning with multiple annotators with different qualities (Zhang & Chaudhuri, 2015; Chen et al., 2022). The primary goal in these work is to identify examples a weak annotator and a strong annotator may disagree, in order to only use the strong annotator on those instances. In our work, we assume access to a single source of annotator that is noisy, which is prevalent in annotation jobs today. Recently, Khosla et al. (2022) proposed a novel deep active learning algorithm specialized for Heteroskedastic noise, where different “regions” of examples are subject to different levels of noise. Unlike their work, our work is agnostic to the noise distributions and conduct experiments on uniformly random corrupted labels.

To the best of our knowledge, no existing deep active learning work has studied the scenario where both imbalance and label noise present. Yet, this setting is the most prevalent in real-world annotation applications.

Agnostic Active Learning A critical part of our solution is the reduction to a one dimensional agnostic active learning problem, e.g. Section 4.1. There is extensive work on agnostic learning in general, and we refer the interested reader to the survey (Hanneke et al., 2014) for a thorough discussion. All of these works, beginning with the seminal works (Balcan et al., 2006; Dasgupta et al., 2007) follow, a familiar paradigm of disagreement based learning. This involves maintainin a version space of promising hypothesis at each time, and constructing the disagreement region as a set of unlabeled examples for which there exists two hypotheses that disagree on their predictions. The example to label is chosen by sampling from a informative sampling distribution computed over the disagreement region. Several approaches have been proposed for computing the sampling distribution, e.g. Jain & Jamieson (2019); Katz-Samuels et al. (2020; 2021); Huang et al. (2015). As described in Section 4.2, our main subroutine VReduce is equivalent to fixed-budget one dimensional threshold disagreement learning based on the ACED algorithm of Katz-Samuels et al.

(2021). We remark that the problem of class imbalance has been largely ignored by the classical work on traditional agnostic learning, and this paper hopes to close this gap.

3. Preliminary

3.1. Notations

We study the pool-based active learning problem, where an initial unlabeled set of N examples $X = \{x_1, \dots, x_N\}$ are available for annotation. Their corresponding labels $Y = \{y_1, \dots, y_N\}$ are initially unknown. Furthermore, we study the multi-class classification problem, where the space of labels $\mathcal{Y} := [K]$ is consisted K classes. Moreover, let N_1, \dots, N_K denote the number of examples in X of each class. We define the imbalance ratio as $\gamma = \frac{\min_{k \in [K]} N_k}{\max_{k' \in [K]} N_{k'}}$.

A deep active learning algorithm iteratively chooses batches of examples for annotation. During the t -th iteration, the algorithm is given labeled and unlabeled sets of examples, L_t and U_t respectively, where $L_t \cup U_t = X$ and $L_t \cap U_t = \emptyset$. The algorithm then chooses B examples from the unlabeled set $X^{(t)} \subseteq U_t$ and then obtains their corresponding labels $Y^{(t)}$. The labeled and unlabeled sets are then updated, i.e., $L_{t+1} \leftarrow L_t \cup X^{(t)}$ and $U_{t+1} \leftarrow U_t \setminus X^{(t)}$. Based on new labeled set L_{t+1} and its corresponding labels, a neural network $f_t : X \rightarrow [K]$ is trained to inform the choice for the next iteration. The ultimate goal of deep active learning is to obtain high predictive accuracy for the trained neural network while annotating as few examples as possible.

3.2. Review of Imbalanced Active Learning: GALAXY

We first consider a binary case of imbalanced classification, where we assume $N_1 < N_2$ without loss of generality. After a total of T rounds and sampling TB examples, random sampling would annotate a subset of X with an imbalance ratio close to $\frac{N_1}{N_2}$. On the other hand, as shown previously in Zhang et al. (2022), uncertainty based methods such as confidence (Settles, 2009), margin (Tong & Koller, 2001; Balcan et al., 2006) and entropy (Kremer et al., 2014) sampling could annotate a set of examples with imbalance ratio arbitrarily low. The reasoning is simply demonstrated in Figure 2a, where choosing examples with predictive sigmoid score \hat{p} closest to .5 may end up annotating examples almost all from the majority class. It is also empirically shown that annotating examples most certain to be in the minority class is not the most effective in improving model performance.

Therefore, the key objective in imbalanced active learning is to label examples that are both *uncertain* and *class balanced*. In both GALAXY (Zhang et al., 2022) and this work, we decompose the objective into the following two-phased procedure:

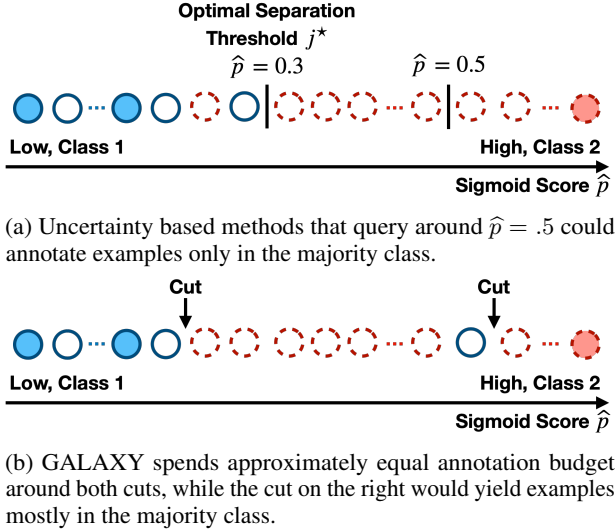


Figure 2: Figures demonstrating GALAXY. Ordered lists of examples are ranked by the predictive sigmoid score \hat{p} . The ground truth label of each example is represented by its border – solid blue lines for class 1 and dotted red lines for class 2. Annotated examples are shaded.

1. Identify the *optimal separation threshold* j^* that best separates the minority class from the majority class, as shown in Figure 2a.
2. Annotate equal number of examples next to j^* from both sides.

GALAXY draws inspiration from graph-based active learning in identifying p^* . In particular, it follows a modified bisection procedure that sequentially annotates examples to find *all* cuts, namely thresholds with a class 1 example to the left and a class 2 example to the right (see Figure 2b). As the optimal separation threshold must be located at one of these cuts, GALAXY annotates examples close to all the found cuts. However, the algorithm suffers from three weaknesses. First, as shown in Figure 2b, by annotating around all cuts, the algorithm may waste a significant portion of the annotation budget around outliers, which could lead to annotating large number of majority class examples. Second, the above problem can be magnified when annotators provide noisy labels. Third, a bisection procedure only allows for sequential labeling, which prevents multiple annotators labeling in parallel. In this paper, we take a DIRECT approach by identifying only the optimal separation threshold and address all of the shortcomings above.

4. A Robust Algorithm with Batch Labeling

In this section, we formally define the optimal separation threshold and pose the problem of identifying it as an 1-dimensional reduction to the agnostic active learning problem. We then propose an algorithm inspired by the agnostic

active learning literature (Balcan et al., 2006; Dasgupta et al., 2007; Hanneke et al., 2014; Katz-Samuels et al., 2021).

4.1. An 1-D Reduction to Agnostic Active Learning

We start by considering the imbalanced binary classification setting mentioned in Section 3.2. When given a neural network model, we let $\hat{p} : X \rightarrow [0, 1]$ be the predictive function mapping examples to sigmoid scores. Here, a higher sigmoid score represents a higher confidence of the example being in class 2. We sort examples by their sigmoid predictive score similar to Section 3.2. Formally, we let $q_{(1)} \leq q_{(2)} \leq \dots \leq q_{(N)}$ be a sorted permutation of $\hat{p}(x_1), \dots, \hat{p}(x_N)$, and let $y_{(1)}, y_{(2)}, \dots, y_{(N)}$ denote the sorted list’s corresponding labels. We are now ready to define the optimal separation threshold as described in Section 3.2.

Definition 4.1. Given a sorting of X the points according the sigmoid scores $0 \leq q_{(1)} \leq \dots \leq q_{(N)} \leq 1$, we define the *optimal separation threshold* as $j^* \in [N]$ such that

$$\begin{aligned} j^* &= \arg \max_j (|\{y_{(i)} = 1 : i \leq j\}| - |\{y_{(i)} = 2 : i \leq j\}|) \\ &= \arg \max_j (|\{y_{(i)} = 2 : i > j\}| - |\{y_{(i)} = 1 : i > j\}|). \end{aligned} \quad (1)$$

In other words, on either side of j^* , it has the largest discrepancy in the number of examples between the two classes. This captures the intuition of Figure 2b — our goal is to find a threshold that best separates one class from the other. We quickly remark that ties are broken by choosing the largest j^* that attains the argmax if class 1 is the minority class and the lowest j^* otherwise.

1D Reduction. We now provide a reduction of finding j^* to an 1-dimensional agnostic active learning problem. We define the hypothesis class $\mathcal{H} = \{h_0, h_1, \dots, h_N\}$ where each hypothesis $h_j : [0, 1] \rightarrow \{1, 2\}$ is defined as

$$h_j(q) = \begin{cases} 1 & \text{if } q \leq q_{(j)} \\ 2 & \text{if } q > q_{(j)} \end{cases}.$$

and $q_{(0)} = 0$ defines the hypothesis h_0 that predicts class 2 at all times. The empirical zero-one loss for each hypothesis is then defined as $\mathcal{L}(h_j) = \sum_{i=1}^N \mathbf{1}\{h_j(q_{(i)}) \neq y_{(i)}\}$. In Appendix A, we show that optimizing for the zero-one loss $\arg \min_{0 \leq j \leq N} \mathcal{L}(h_j)$ is equivalent to (1). Namely, $j^* \in \arg \min_{0 \leq j \leq N} \mathcal{L}(h_j)$, transforming the problem of finding the optimal separation threshold to an 1-D agnostic active learning problem.

Multi-Class Classification. To generalize the above problem formulation to multi-class classification, we follow a similar strategy to Zhang et al. (2022). Specifically, for each class k , one can view the problem of class- k v.s. others as a

Algorithm 1 DIRECT: DIMension REDuction for aCTive Learning under Imbalance and Label Noise

Input: Pool X , number of rounds T , retraining batch size B_{train} , number of parallel annotations B_{parallel} .

Initialize: Uniformly sample B elements without replacement from X to form L_0 . Let $U_0 \leftarrow X \setminus L_0$.

for $t = 1, \dots, T - 1$ **do**

Train neural network on L_{t-1} and obtain f_{t-1} .

Find optimal separation thresholds

Initialize labeled set $L_t \leftarrow L_{t-1}$.

Initialize budget per class $b \leftarrow B_{\text{train}}/2K$.

for k in $\text{RandPerm}(\{1, \dots, K\})$ **do**

Compute margin scores q_1^k, \dots, q_N^k based on f_{t-1} and sort them by $q_{(1)}^k \leq \dots \leq q_{(N)}^k$ and break ties so that $q_{(i)}^k = q_{(i+1)}^k \implies [\widehat{p}(x_{(i)})]_k \geq [\widehat{p}(x_{(i+1)})]_k$.

Find optimal separation threshold: $L_t \leftarrow \text{VReduce}(L_t, b, k, B_{\text{parallel}}, \{q_{(i)}^k\}_{i=1}^N)$.

end for

Annotate rare and uncertain examples

Compute budget per class $b \leftarrow (B_{\text{train}} - |L_t|)/K$.

for k in $\text{RandPerm}(\{1, \dots, K\})$ **do**

Estimate separation threshold

$$\widehat{j}^k \leftarrow \arg \max_j (|\{y_{(i)} = 1 : x_{(i)} \in L_t \text{ and } i \leq j\}| - |\{y_{(i)} = 1 : x_{(i)} \in L_t \text{ and } i \leq j\}|)$$

and break ties by choosing the index closest to $\frac{N}{2}$.

Annotate b unlabeled examples with sorted indices closest to \widehat{j}^k and insert to L_t .

end for

end for

Return: Train final classifier f_T based on L_T .

binary classification problem. In other words, class k can be seen as class 1 and classes $\{1, \dots, k - 1, k + 1, \dots, N\}$ can be seen as class 2. The goal therefore becomes finding all K optimal separation thresholds, which is equivalent with solving K 1-D agnostic active learning problems. Moreover, let $\widehat{p} : X \rightarrow \Delta^{(K-1)}$ denote the neural network prediction function mapping examples to sigmoid scores. Instead of using sigmoid scores, for class k , we use the margin scores $q_i^k := \max_{k'} [\widehat{p}(x_i)]_{k'} - [\widehat{p}(x_i)]_k$ to sort the examples. When multiple examples have the same margin score, we further break ties by their corresponding confidence scores $[\widehat{p}(x_i)]_k$. We also note that sorting with margin scores is equivalent to sorting with sigmoid scores in the binary classification setting, so this is a strictly more general formulation to multi-class classification.

4.2. Algorithm

We are now ready to state our algorithm as shown in Algorithm 1. The algorithm follows a two-phased procedure,

Algorithm 2 VReduce: Version Space Reduction

Input: Labeled set L , budget b , class of interest k , parallel batch size B_{parallel} , examples and ground truth labels sorted by uncertainty $\{q_{(i)}\}_{i=1}^N$.

Define: For examples in the labeled set, we let $y_{(i)}$ denote the label of the example corresponding to $q_{(i)}$.

Initialize: Version space: shortest segment of indices $[I, J]$, with $q_{(I)}, q_{(J)} \forall i \leq I, q_{(i)} \in L \implies y_{(i)} = k$ and $\forall j \geq J, q_{(j)} \in L \implies y_{(j)} \neq k$.

Initialize: Number of iterations $m \leftarrow \frac{b}{B_{\text{parallel}}}$. Shrinking factor $c \leftarrow \sqrt[m]{J - I}$.

for $t = 1, \dots, m$ **do**

Sample uniformly at random B_{parallel} unlabeled examples in $q_{(I)}, \dots, q_{(J)}$ for annotation and insert to L .

Find $[I', J'] \subset [I, J]$ such that

$$I', J' = \arg \min_{i, j: j-i = \frac{1}{c}(J-I)} \max\{\widehat{\mathcal{L}}^k(i), \widehat{\mathcal{L}}^k(j)\} \text{ where}$$

$$\widehat{\mathcal{L}}^k(s) = \sum_{\substack{r \leq s: \\ q_{(r)} \in L}} \mathbf{1}\{y_{(r)} \neq k\} + \sum_{\substack{r > s: \\ q_{(r)} \in L}} \mathbf{1}\{y_{(r)} = k\}.$$

Update version space $I, J \leftarrow I', J'$.

end for

Return: Updated labeled set L .

where the first phase aims to identify the optimal separation threshold for each class. The second phase then annotates examples closest to the estimated optimal separation thresholds for each class. Our set of labeled examples at anytime are maintained in L_t .

To identify the optimal separation threshold, we loop over each class k and run a fix-budget batch active learning procedure for the one-dimensional reduction (as shown in Algorithm 2) on the set of labeled examples. Our method is motivated by the fixed-budget algorithm for active classification, ACED (Katz-Samuels et al., 2021). Intuitively, in the non-noisy or separable setting, where the loss of $\mathcal{L}(h_{j^*}) = 0$, we could run a binary search procedure to learn j^* . However, we can't assume that j^* perfectly separates the classes. ACED circumvents this by maintaining a version space of threshold classifiers, namely an interval $[I, J]$. In each of the b/B_{parallel} rounds, B_{parallel} samples are taken and appended to the set of labeled examples L . Then, an interval I', J' is computed, whose length is a factor of $1/c$ smaller than the current I, J of low-loss classifiers. The shrinkage rate c is determined by the budget and batch size, so that after the final iteration, the version space has exactly one hypothesis left. The fixed confidence (or alternatively δ -PAC) analogue of ACED is known to match instance optimal lower bounds for active classification up to logarithmic factors. Under benign noise conditions, the probability of misidentifying

the optimal separation threshold decays exponentially w.r.t. budget b .

To address batch labeling, we note the number of examples collected before retraining is usually far greater than the number of annotators annotating in parallel. In particular, we let B_{train} denote the number of examples the algorithm collects before the neural network is retrained. In practice, this number is usually determined by the constraints of computational training cost. On the other hand, we let B_{parallel} denote the number of examples annotated in parallel. As discussed above, $B_{\text{parallel}} \ll B_{\text{train}}$ in practice. Lastly, as will be discussed in Section 6, a variant of our algorithm can also be proposed for asynchronous labeling.

5. Experiments

We conduct experiments under two primary setups:

1. Fine-tuning ResNet-18 with vanilla supervised training on imbalanced datasets similar to Zhang et al. (2022).
2. Fine-tuning large pretrained model (CLIP ViT-B32) with semi-supervised training strategies under the LabelBench framework (Zhang et al., 2023a).

In Section 5.1, we document these setups in detail. For both evaluation setups, we first evaluate the performance of DIRECT under the noiseless setting in Section 5.2, showing its superior label-efficiency and ability to accommodate batch labeling. In Section 5.3, we evaluate deep active learning algorithms under a novel setting with both class imbalance and noisy labels. Under this setting, we also include an ablation study of the performance of DIRECT on various levels of label noises. While we highlight many results in this section, see Appendix B for all results.

5.1. Experiment Setup

ResNet-18 Experiments. ResNet-18 with passive training has been the standard evaluation in existing deep active literature (Ash et al., 2019; Zhang et al., 2022). Our experiment setup utilizes the CIFAR-10, CIFAR-100 (Krizhevsky et al., 2009), SVHN (Netzer et al., 2011) and PathMNIST (Yang et al., 2021) image classification datasets. The original forms of these datasets are roughly balanced across 9, 10 or 100 classes. We construct an extremely imbalanced dataset by grouping a large number of classes into one majority class. For example, given a balanced dataset above with M classes. We generate an imbalanced dataset with K classes ($K < M$) by the first $K - 1$ classes from the original dataset and combining the rest of the classes K, \dots, M into a single majority class K . Imbalance ratios are shown in Table 1.

For neural network training, we utilize the standard passive training on labeled examples with cross entropy loss and Adam optimizer (Kingma & Ba, 2014). The ResNet-18

Name	# Classes K	N	Imb Ratio $\gamma = \frac{\min_k N_k}{\max_{k'} N_{k'}}$
Imb CIFAR-10	2	50000	.1111
Imb CIFAR-10	3	50000	.1250
Imb CIFAR-100	2	50000	.0101
Imb CIFAR-100	3	50000	.0102
Imb CIFAR-100	10	50000	.0110
Imb SVHN	2	73257	.0724
Imb SVHN	3	54448	.2546
PathMNIST	2	89996	.1166
FMoW	62	76863	.0049
iWildCam	14	129809	$4.57 \cdot 10^{-5}$

Table 1: Dataset settings for our experiments. N denotes the total number of examples in our dataset. γ is the class imbalance ratio defined in Section 3.1.

model (He et al., 2016) is pretrained on ImageNet (Deng et al., 2009) from the PyTorch library. To address data imbalance, we utilize a reweighted cross entropy loss by the inverse frequency of the number of labeled examples in each class. For experiments with label noise, we further add a 10% label smoothing during training (Müller et al., 2019).

LabelBench Experiments. Proposed by Zhang et al. (2023a), LabelBench evaluates active learning performance in a more comprehensive framework. Here, we fine-tune the large pretrained model from CLIP’s ViT-B32 model (Radford et al., 2021). The framework also utilizes semi-supervised learning method FlexMatch (Zhang et al., 2021) to further leverage the unlabeled examples in the pool for training. We conduct experiments on the two imbalanced datasets in LabelBench, with FMoW (Christie et al., 2018) and iWildcam (Beery et al., 2021). Similar to the ResNet-18 experiments, we use a 10% label smoothing in the loss function to improve training under label noise. We did find FlexMatch to perform poorly under the combination of imbalance and label noise, so we used the passive training method for label noise experiments.

5.2. Experiments under Imbalance, without Label Noise

For the noiseless experiment on ResNet-18, we compare against nine baselines: GALAXY (Zhang et al., 2022), SIMILAR (Kothawade et al., 2021), BADGE (Ash et al., 2019), BASE (Emam et al., 2021), BAIT (Ash et al., 2021), Cluster Margin (Citovsky et al., 2021), Confidence Sampling (Settles, 2009), Most Likely Positive (Jiang et al., 2018; Warmuth et al., 2001; 2003) and Random Sampling. We briefly distinguish the algorithms into two categories. In particular, both SIMILAR and Most Likely Positive annotate examples that are similar to existing labeled minority examples, thus can significantly annotate a large quantity of minority examples. The rest of the algorithms primarily optimizes for different notions of informativeness such as diversity and uncertainty. For the LabelBench experiments, due to the large

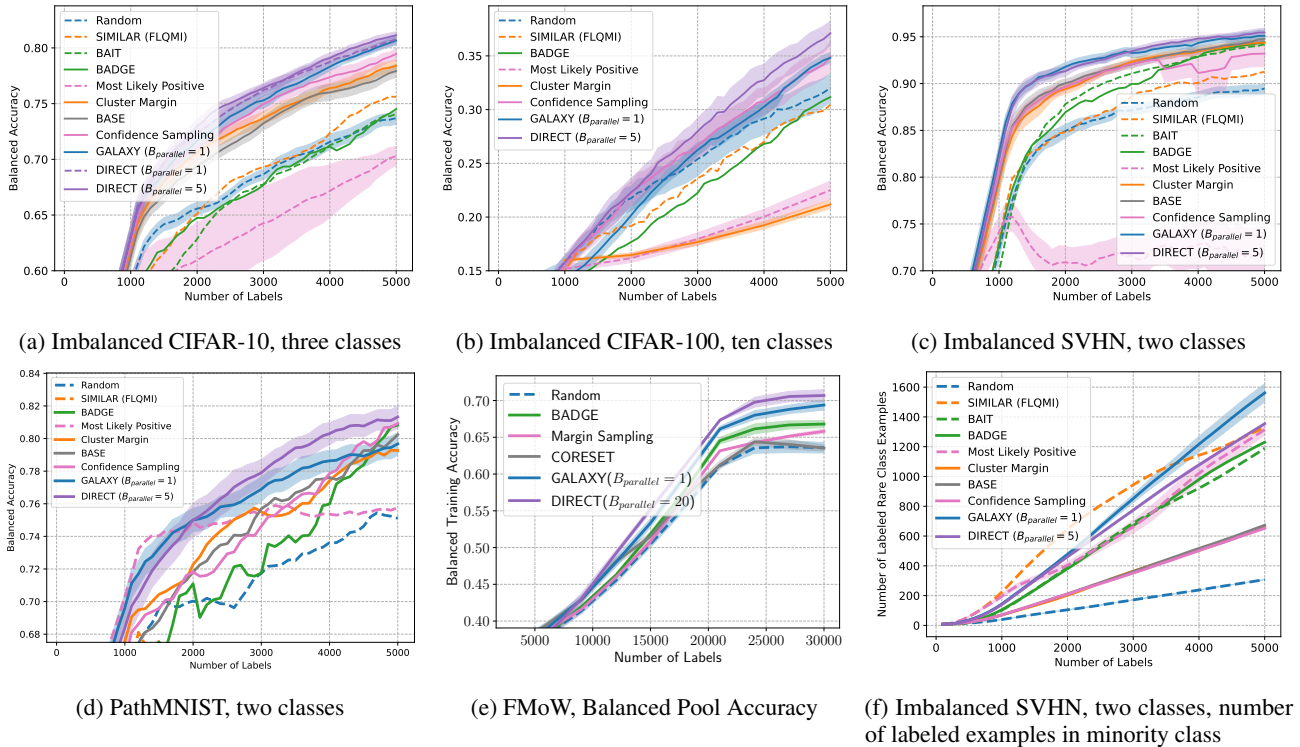


Figure 3: Performance comparison of DIRECT against other baselines algorithms in the noiseless but imbalanced setting. (a)-(d) are balanced accuracy on ResNet-18 experiments while (e) shows experiment under the LabelBench framework. B_{parallel} indicates the number of parallel annotations as mentioned in Section 4.2. $B_{\text{parallel}} = 1$ is equivalent with synchronous labeling. Results are averaged over four trials and the shaded areas represent standard errors around the average performances.

dataset and model embedding sizes, we choose a subset of the algorithms that are computationally efficient and among top performers in the ResNet-18 results. In particular, we compared against BADGE, Margin Sampling (Balcan et al., 2006; Kremer et al., 2014), CORESET and GALAXY.

As highlighted in Figures 1(a) and 3(a)-(d), DIRECT consistently and significantly outperforms existing algorithms on the ResNet-18 experiments. In Figures 1(c) and 3(e), we demonstrate the increased label-efficiency is also consistently shown in the LabelBench experiments. Compared to random sampling, DIRECT can save more than 80% of the annotation cost on imbalanced SVHN experiment of Figure 3(c). In terms of class-balancedness, we consistently observe that both Most Likely Positive and SIMILAR annotating greater number of minority class examples, but significantly underperforms in terms of balanced accuracy (an example shown in Figure 3(f)). While Zhang et al. (2022) has already observed this phenomenon, we can further see that DIRECT collects slightly less minority class examples than GALAXY, but outperforms in terms of balanced accuracy. While it is crucial to optimize class-balancedness for better model performance, we see that both extremes of annotating too few and too many minority examples could

lead to worse generalization performances. When too few examples are from minority class, the performance of the minority classes could be significantly hindered. When optimized to annotate as many examples from minority class as possible, the algorithm has to tradeoff annotating informative examples to examples it is more certain to be in the minority class. Together, this suggests an intricate balance between the two objectives, generalization performance and class-balancedness.

We would also like to highlight the ability to handle batch labeling. Across our experiments, we see DIRECT outperforms with different amounts of parallel annotation ($B_{\text{parallel}} = 1, 5$ and 20), indicating its general effectiveness. This is in comparison to the synchronous nature of GALAXY, where it is always using $B_{\text{parallel}} = 1$. On Figures 1(a) and 4(a), we see that DIRECT outperforms GALAXY with synchronous labeling. Furthermore, in these experiments we also see using $B_{\text{parallel}} = 5$ only affects algorithm performances minimally for DIRECT.

5.3. Experiments under Imbalance and Label Noise

We conduct novel sets of experiments under both class imbalance and label noise. Here, for both ResNet-18 and

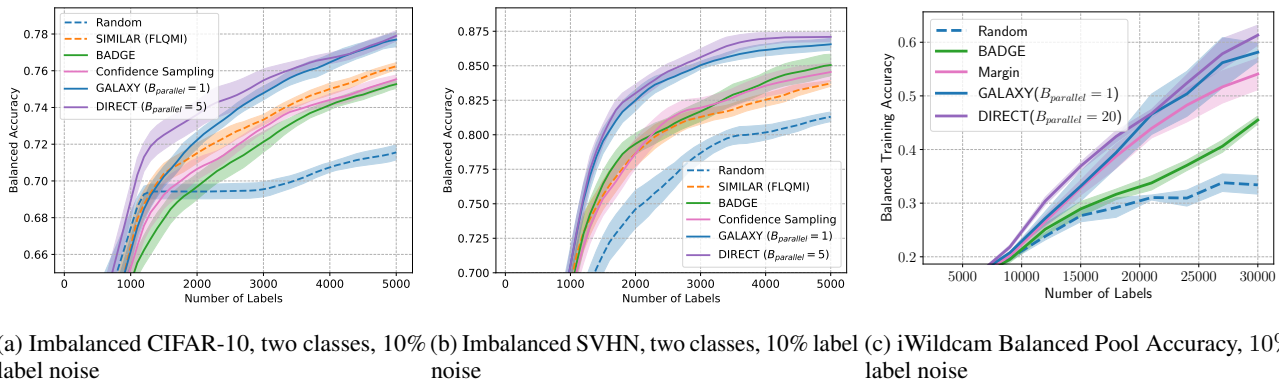


Figure 4: Performance of DIRECT against baseline algorithms under 10% label noise. (a)-(b) are balanced accuracy on ResNet-18 experiments while (c) shows results under the LabelBench framework. Results are averaged over four trials and the shaded areas represent standard errors around the average performances.

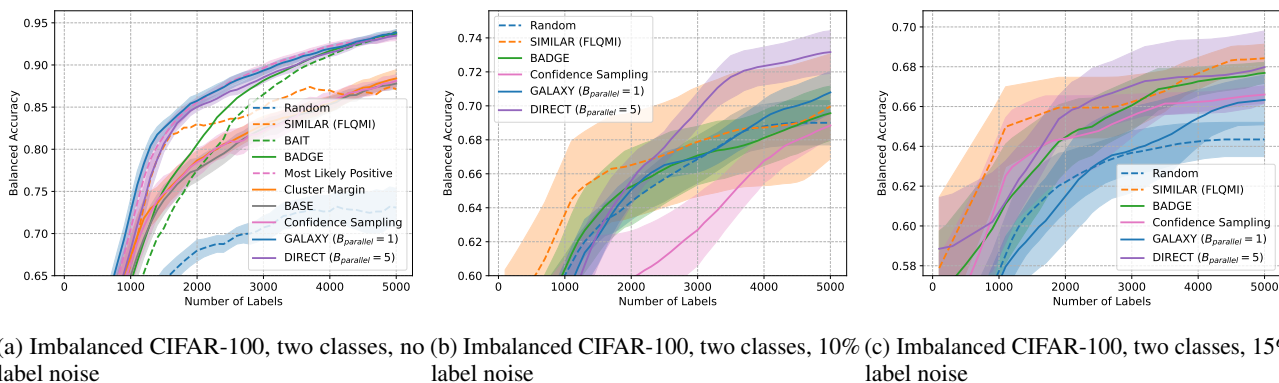


Figure 5: Performance of DIRECT against baseline algorithms under different levels of label noise. Results are averaged over four trials and the shaded areas represent standard errors around the average performances.

LabelBench experiments, we evaluate against all of the algorithms that performed well under the imbalance but noiseless setting above. For all of our experiments, we introduce a fixed percentage of label noise, where the given fraction of the examples’ labels are corrupted to a different class uniformly at random. For most of our experiments with 10% label noise shown in Figure 4, we observe again that DIRECT consistently improves over all baselines including GALAXY. The results are consistent on ResNet-18 and LabelBench setups, and with different B_{parallel} values, showing DIRECT’s robustness under label noise.

Different Levels of Label Noise As shown in Figures 5(a)-(c) and 1(b), we observe the results on imbalanced CIFAR-100 with two classes across numerous levels of label noise, with 0%, 10%, 15% and 20% respectively. In fact, the noiseless experiment in Figure 5(a) is the only setting DIRECT slightly underperforms GALAXY in terms of generalization accuracy. However, we see DIRECT becomes more label-efficient under the more practical label noise settings. It is also worth noting that with high label noise of 20%,

we observe in Figure 1(b) that existing algorithms underperform random sampling. In contrast, DIRECT significantly outperforms random sampling, saving more than 60% of the annotation cost.

6. Conclusion and Future Work

In this paper, we conducted the first study of deep active learning under both class imbalance and label noise. We proposed an algorithm DIRECT that significantly and consistently outperforms existing literature. In this work, we also addressed the batch sampling problem of current SOTA algorithm, GALAXY (Zhang et al., 2022), by annotating multiple examples in parallel. Studying asynchronous labeling could be a natural extension of our work. We think a potential solution is to utilize an asynchronous variant of one-dimensional active learning algorithm. In addition, one can further batch the labeling process across different classes to further accommodate an even larger number of parallel annotators.

Acknowledgements

This work has been supported in part by NSF Award 2112471.

Impact Statement

In the rapidly evolving landscape of machine learning, the efficacy of active learning in addressing data imbalance and label noise is a significant stride towards more robust and equitable AI systems. This research explores how active learning can effectively mitigate the challenges posed by imbalanced datasets and erroneous labels, prevalent in real-world scenarios.

The positive impacts of this research are multifaceted. It enhances the accessibility and utility of machine learning in domains where data imbalance is a common challenge, such as healthcare, finance, and social media analytics. By improving class-balancedness in annotated sets, models trained on these datasets are less biased and more representative of real-world distributions, leading to fairer and more accurate outcomes. Additionally, this research contributes to reducing the time and cost associated with data annotation, which is particularly beneficial in fields where expert annotation is expensive or scarce.

However, if not carefully implemented, active learning strategies could inadvertently introduce new biases or amplify existing ones, particularly in scenarios where the initial data is severely imbalanced or contains deeply ingrained biases. Furthermore, the advanced nature of these techniques may widen the gap between organizations with access to state-of-the-art technology and those without, potentially exacerbating existing inequalities in technology deployment.

References

- Aggarwal, U., Popescu, A., and Hudelot, C. Active learning for imbalanced datasets. In *Proceedings of the IEEE/CVF Winter Conference on Applications of Computer Vision*, pp. 1428–1437, 2020.
- Ash, J., Goel, S., Krishnamurthy, A., and Kakade, S. Gone fishing: Neural active learning with fisher embeddings. *Advances in Neural Information Processing Systems*, 34: 8927–8939, 2021.
- Ash, J. T., Zhang, C., Krishnamurthy, A., Langford, J., and Agarwal, A. Deep batch active learning by diverse, uncertain gradient lower bounds. *arXiv preprint arXiv:1906.03671*, 2019.
- Balcan, M.-F., Beygelzimer, A., and Langford, J. Agnostic active learning. In *Proceedings of the 23rd international conference on Machine learning*, pp. 65–72, 2006.
- Beery, S., Agarwal, A., Cole, E., and Birodkar, V. The iwildcam 2021 competition dataset. *arXiv preprint arXiv:2105.03494*, 2021.
- Beluch, W. H., Genewein, T., Nürnberger, A., and Köhler, J. M. The power of ensembles for active learning in image classification. In *Proceedings of the IEEE conference on computer vision and pattern recognition*, pp. 9368–9377, 2018.
- Cai, X. Active learning for imbalanced data: The difficulty and proportions of class matter. *Wireless Communications and Mobile Computing*, 2022, 2022.
- Chen, Y., Sankararaman, K., Lazaric, A., Pirota, M., Karamshuk, D., Wang, Q., Mandyam, K., Wang, S., and Fang, H. Improved adaptive algorithm for scalable active learning with weak labeler. *arXiv preprint arXiv:2211.02233*, 2022.
- Christie, G., Fendley, N., Wilson, J., and Mukherjee, R. Functional map of the world. In *Proceedings of the IEEE Conference on Computer Vision and Pattern Recognition*, pp. 6172–6180, 2018.
- Citovsky, G., DeSalvo, G., Gentile, C., Karydas, L., Rajagopalan, A., Rostamizadeh, A., and Kumar, S. Batch active learning at scale. *Advances in Neural Information Processing Systems*, 34:11933–11944, 2021.
- Coleman, C., Chou, E., Katz-Samuels, J., Culatana, S., Bailis, P., Berg, A. C., Nowak, R., Sumbaly, R., Zaharia, M., and Yalniz, I. Z. Similarity search for efficient active learning and search of rare concepts. In *Proceedings of the AAAI Conference on Artificial Intelligence*, volume 36, pp. 6402–6410, 2022.
- Dasgupta, S., Hsu, D. J., and Monteleoni, C. A general agnostic active learning algorithm. *Advances in neural information processing systems*, 20, 2007.
- Deng, J., Dong, W., Socher, R., Li, L.-J., Li, K., and Fei-Fei, L. Imagenet: A large-scale hierarchical image database. In *2009 IEEE conference on computer vision and pattern recognition*, pp. 248–255. Ieee, 2009.
- Ducoffe, M. and Precioso, F. Adversarial active learning for deep networks: a margin based approach. *arXiv preprint arXiv:1802.09841*, 2018.
- Elenter, J., NaderiAlizadeh, N., and Ribeiro, A. A lagrangian duality approach to active learning. *arXiv preprint arXiv:2202.04108*, 2022.
- Emam, Z. A. S., Chu, H.-M., Chiang, P.-Y., Czaja, W., Leapman, R., Goldblum, M., and Goldstein, T. Active learning at the imagenet scale. *arXiv preprint arXiv:2111.12880*, 2021.

- Gal, Y., Islam, R., and Ghahramani, Z. Deep bayesian active learning with image data. In *International Conference on Machine Learning*, pp. 1183–1192. PMLR, 2017.
- Geifman, Y. and El-Yaniv, R. Deep active learning over the long tail. *arXiv preprint arXiv:1711.00941*, 2017.
- Hanneke, S. et al. Theory of disagreement-based active learning. *Foundations and Trends® in Machine Learning*, 7(2-3):131–309, 2014.
- He, K., Zhang, X., Ren, S., and Sun, J. Deep residual learning for image recognition. In *Proceedings of the IEEE conference on computer vision and pattern recognition*, pp. 770–778, 2016.
- Huang, T.-K., Agarwal, A., Hsu, D. J., Langford, J., and Schapire, R. E. Efficient and parsimonious agnostic active learning. *Advances in Neural Information Processing Systems*, 28, 2015.
- Jain, L. and Jamieson, K. G. A new perspective on pool-based active classification and false-discovery control. *Advances in Neural Information Processing Systems*, 32, 2019.
- Jiang, S., Malkomes, G., Abbott, M., Moseley, B., and Garnett, R. Efficient nonmyopic batch active search. In *32nd Conference on Neural Information Processing Systems (NeurIPS 2018)*, 2018.
- Jin, Q., Yuan, M., Wang, H., Wang, M., and Song, Z. Deep active learning models for imbalanced image classification. *Knowledge-Based Systems*, 257:109817, 2022.
- Katz-Samuels, J., Jain, L., Jamieson, K. G., et al. An empirical process approach to the union bound: Practical algorithms for combinatorial and linear bandits. *Advances in Neural Information Processing Systems*, 33:10371–10382, 2020.
- Katz-Samuels, J., Zhang, J., Jain, L., and Jamieson, K. Improved algorithms for agnostic pool-based active classification. In *International Conference on Machine Learning*, pp. 5334–5344. PMLR, 2021.
- Khosla, S., Whye, C. K., Ash, J. T., Zhang, C., Kawaguchi, K., and Lamb, A. Neural active learning on heteroskedastic distributions. *arXiv preprint arXiv:2211.00928*, 2022.
- Kingma, D. P. and Ba, J. Adam: A method for stochastic optimization. *arXiv preprint arXiv:1412.6980*, 2014.
- Kothawade, S., Beck, N., Killamsetty, K., and Iyer, R. Similar: Submodular information measures based active learning in realistic scenarios. *Advances in Neural Information Processing Systems*, 34:18685–18697, 2021.
- Kremer, J., Steenstrup Pedersen, K., and Igel, C. Active learning with support vector machines. *Wiley Interdisciplinary Reviews: Data Mining and Knowledge Discovery*, 4(4):313–326, 2014.
- Krizhevsky, A., Hinton, G., et al. Learning multiple layers of features from tiny images. 2009.
- Lin, C., Mausam, M., and Weld, D. Re-active learning: Active learning with relabeling. In *Proceedings of the AAAI Conference on Artificial Intelligence*, volume 30, 2016.
- Mohamadi, M. A., Bae, W., and Sutherland, D. J. Making look-ahead active learning strategies feasible with neural tangent kernels. *arXiv preprint arXiv:2206.12569*, 2022.
- Müller, R., Kornblith, S., and Hinton, G. E. When does label smoothing help? *Advances in neural information processing systems*, 32, 2019.
- Netzer, Y., Wang, T., Coates, A., Bissacco, A., Wu, B., and Ng, A. Y. Reading digits in natural images with unsupervised feature learning. 2011.
- Radford, A., Kim, J. W., Hallacy, C., Ramesh, A., Goh, G., Agarwal, S., Sastry, G., Askell, A., Mishkin, P., Clark, J., et al. Learning transferable visual models from natural language supervision. In *International conference on machine learning*, pp. 8748–8763. PMLR, 2021.
- Sener, O. and Savarese, S. Active learning for convolutional neural networks: A core-set approach. *arXiv preprint arXiv:1708.00489*, 2017.
- Settles, B. Active learning literature survey. 2009.
- Tong, S. and Koller, D. Support vector machine active learning with applications to text classification. *Journal of machine learning research*, 2(Nov):45–66, 2001.
- Wang, H., Huang, W., Margenot, A., Tong, H., and He, J. Deep active learning by leveraging training dynamics. *arXiv preprint arXiv:2110.08611*, 2021.
- Warmuth, M. K., Rätsch, G., Mathieson, M., Liao, J., and Lemmen, C. Active learning in the drug discovery process. In *NIPS*, pp. 1449–1456, 2001.
- Warmuth, M. K., Liao, J., Rätsch, G., Mathieson, M., Putta, S., and Lemmen, C. Active learning with support vector machines in the drug discovery process. *Journal of chemical information and computer sciences*, 43(2):667–673, 2003.
- Yang, J., Shi, R., Wei, D., Liu, Z., Zhao, L., Ke, B., Pfister, H., and Ni, B. Medmnist v2: A large-scale lightweight benchmark for 2d and 3d biomedical image classification. *arXiv preprint arXiv:2110.14795*, 2021.

- Younesian, T., Zhao, Z., Ghiassi, A., Birke, R., and Chen, L. Y. Qactor: Active learning on noisy labels. In *Asian Conference on Machine Learning*, pp. 548–563. PMLR, 2021.
- Zhang, B., Wang, Y., Hou, W., Wu, H., Wang, J., Okumura, M., and Shinozaki, T. Flexmatch: Boosting semi-supervised learning with curriculum pseudo labeling. *Advances in Neural Information Processing Systems*, 34: 18408–18419, 2021.
- Zhang, C. and Chaudhuri, K. Active learning from weak and strong labelers. *Advances in Neural Information Processing Systems*, 28, 2015.
- Zhang, J., Katz-Samuels, J., and Nowak, R. Galaxy: Graph-based active learning at the extreme. *arXiv preprint arXiv:2202.01402*, 2022.
- Zhang, J., Chen, Y., Canal, G., Mussmann, S., Zhu, Y., Du, S. S., Jamieson, K., and Nowak, R. D. Label-bench: A comprehensive framework for benchmarking label-efficient learning. *arXiv preprint arXiv:2306.09910*, 2023a.
- Zhang, J., Shao, S., Verma, S., and Nowak, R. Algorithm selection for deep active learning with imbalanced datasets. *arXiv preprint arXiv:2302.07317*, 2023b.

A. Equivalent Objective

Lemma A.1. *The agnostic active learning reduction is equivalently finding the optimal separation threshold. Namely,*

$$\arg \min_j \mathcal{L}(h_j) = \arg \max_j (|\{y_{(i)} = 1 : 1 \leq i \leq j\}| - |\{y_{(i)} = 2 : 1 \leq i \leq j\}|)$$

Proof. Recall the definitions: $h_j(q) = \begin{cases} 1 & \text{if } q \leq q_{(j)} \\ 2 & \text{if } q > q_{(j)} \end{cases}$ and $\mathcal{L}(h_j) = \sum_{i=1}^N \mathbf{1}\{h_j(q_{(i)}) \neq y_{(i)}\}$, we can expand the loss as follows

$$\begin{aligned} \arg \min_j \mathcal{L}(h_j) &= \arg \min_j \sum_{i=1}^N \mathbf{1}\{h_j(q_{(i)}) \neq y_{(i)}\} \\ &= \arg \min_j N - \sum_{i=1}^N \mathbf{1}\{h_j(q_{(i)}) = y_{(i)}\} \\ &= \arg \max_j \sum_{i=1}^N \mathbf{1}\{h_j(q_{(i)}) = y_{(i)}\} \\ &= \arg \max_j \left(\sum_{i=1}^j \mathbf{1}\{y_{(i)} = 1\} \right) + \left(\sum_{i=j+1}^N \mathbf{1}\{y_{(i)} = 2\} \right) \\ &= \arg \max_j \left(\sum_{i=1}^j \mathbf{1}\{y_{(i)} = 1\} \right) + \left(\sum_{i=j+1}^N \mathbf{1}\{y_{(i)} = 2\} \right) - \left(\sum_{i=1}^N \mathbf{1}\{y_{(i)} = 2\} \right) \\ &= \arg \max_j \sum_{i=1}^j (\mathbf{1}\{y_{(i)} = 1\} - \mathbf{1}\{y_{(i)} = 2\}) \end{aligned}$$

□

B. All Results

B.1. Noiseless Results under Imbalance

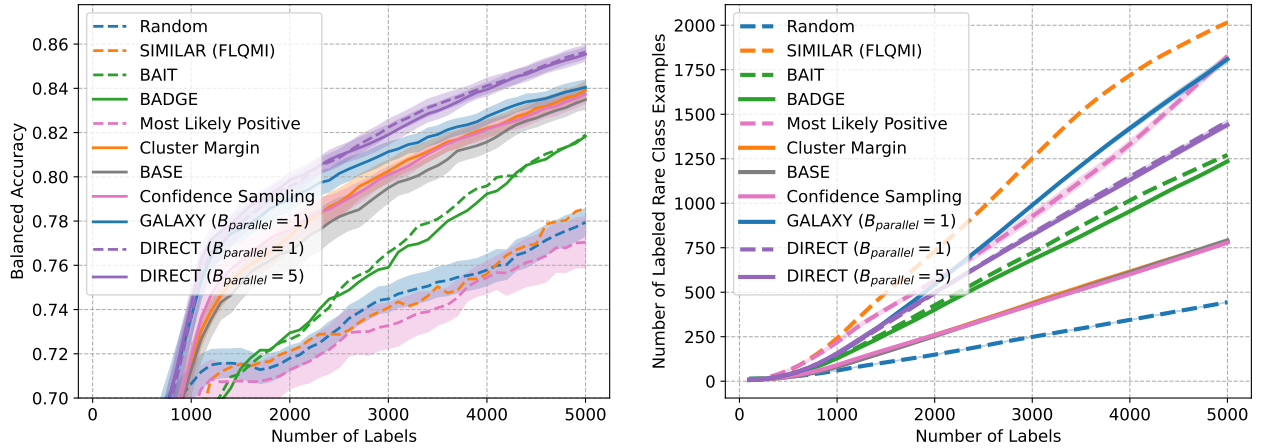


Figure 6: Imbalanced CIFAR-10, two classes.

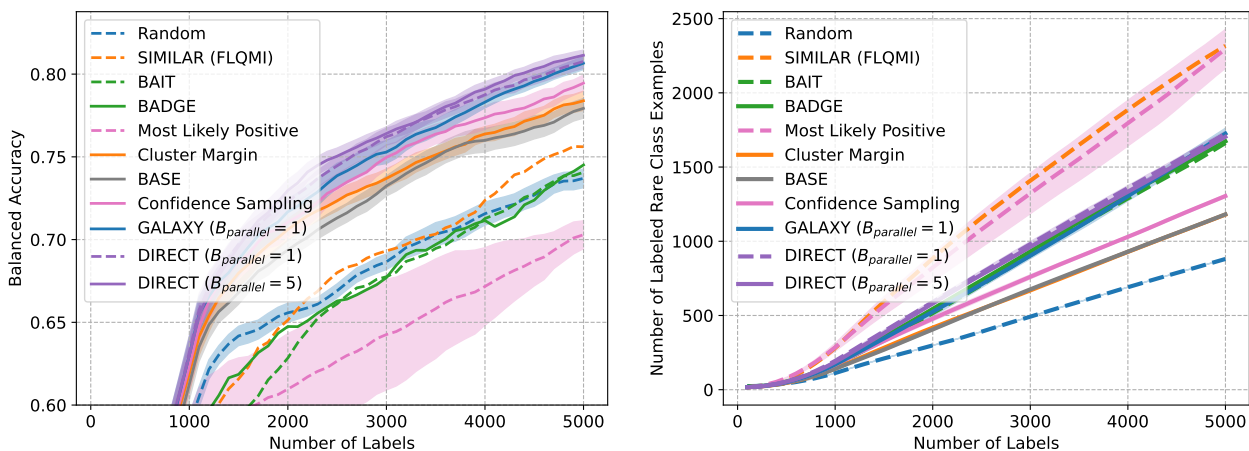


Figure 7: Imbalanced CIFAR-10, three classes.

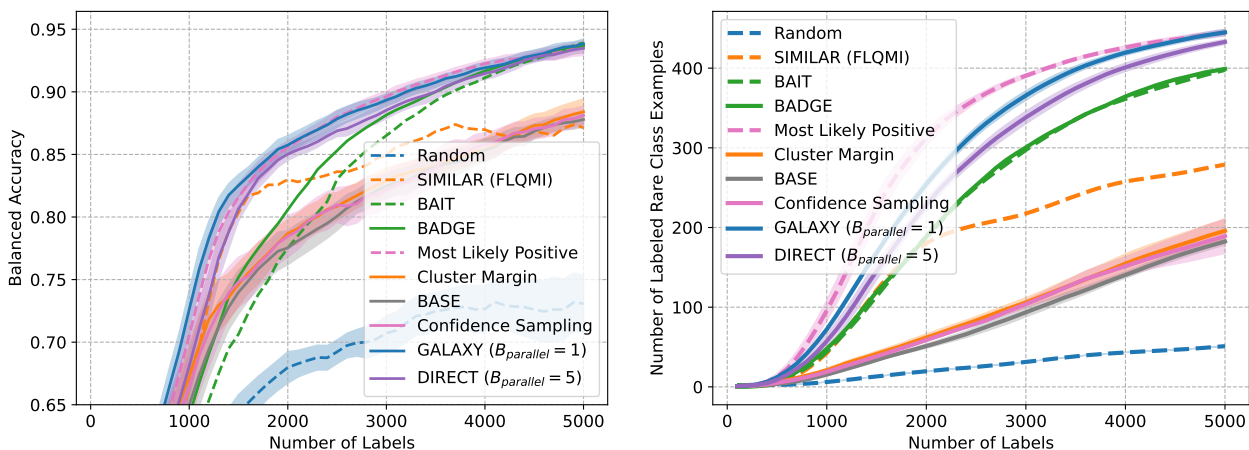


Figure 8: Imbalanced CIFAR-100, two classes.

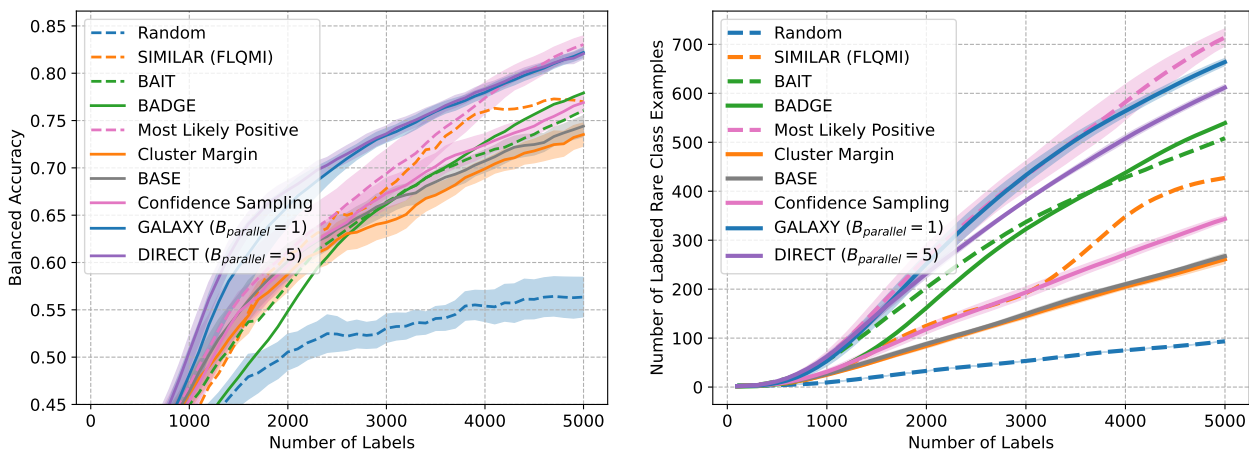


Figure 9: Imbalanced CIFAR-100, three classes.

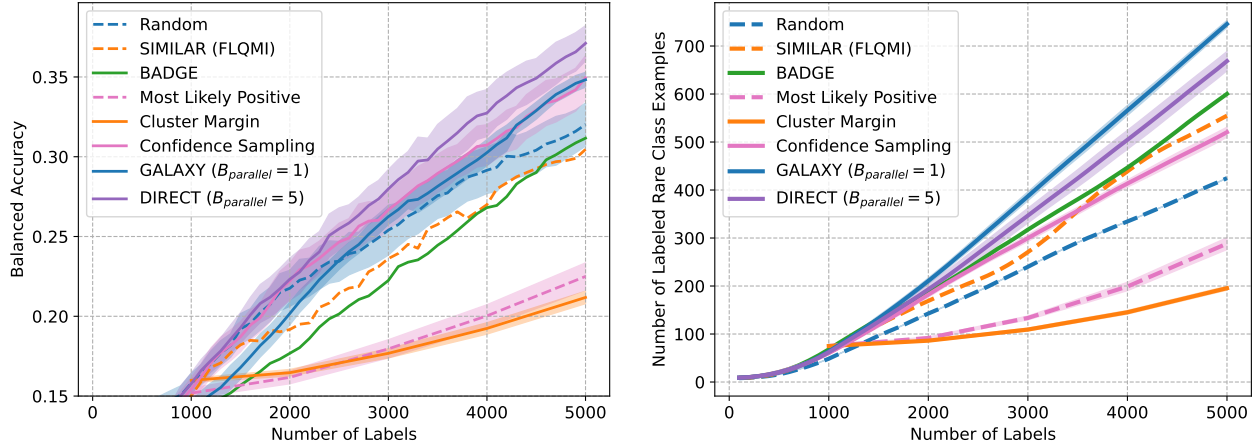


Figure 10: Imbalanced CIFAR-100, 10 classes.

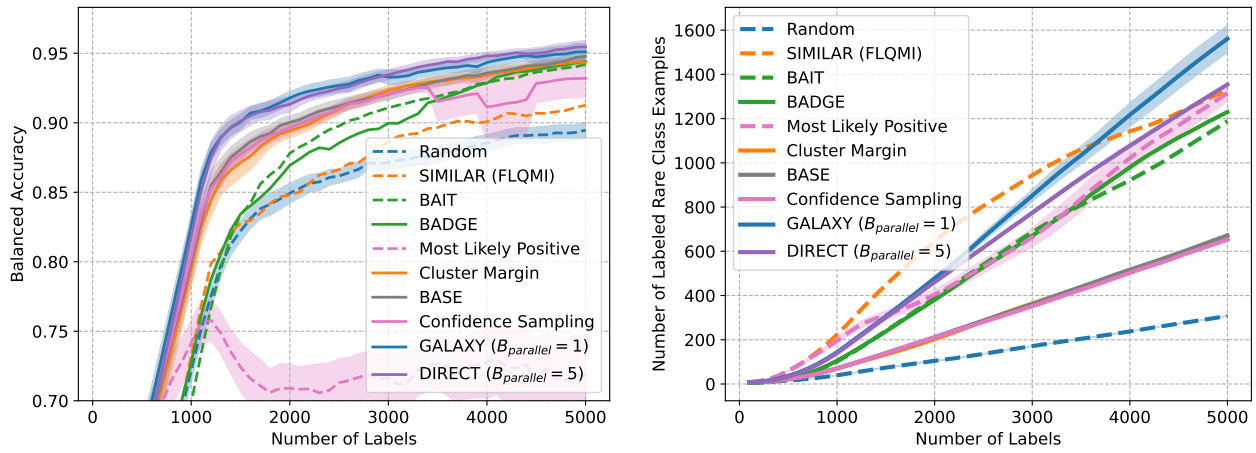


Figure 11: Imbalanced SVHN, two classes.

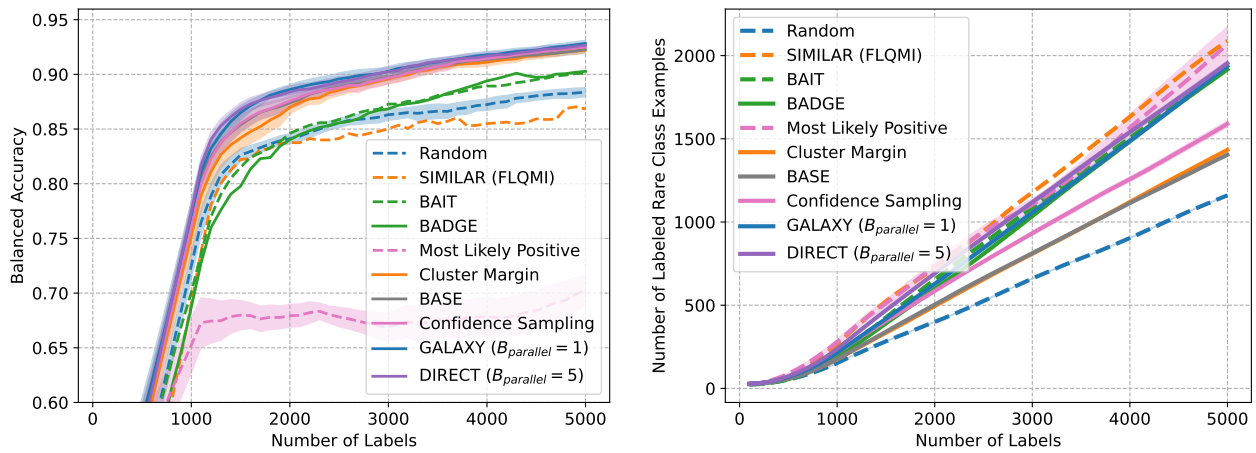


Figure 12: Imbalanced SVHN, three classes.

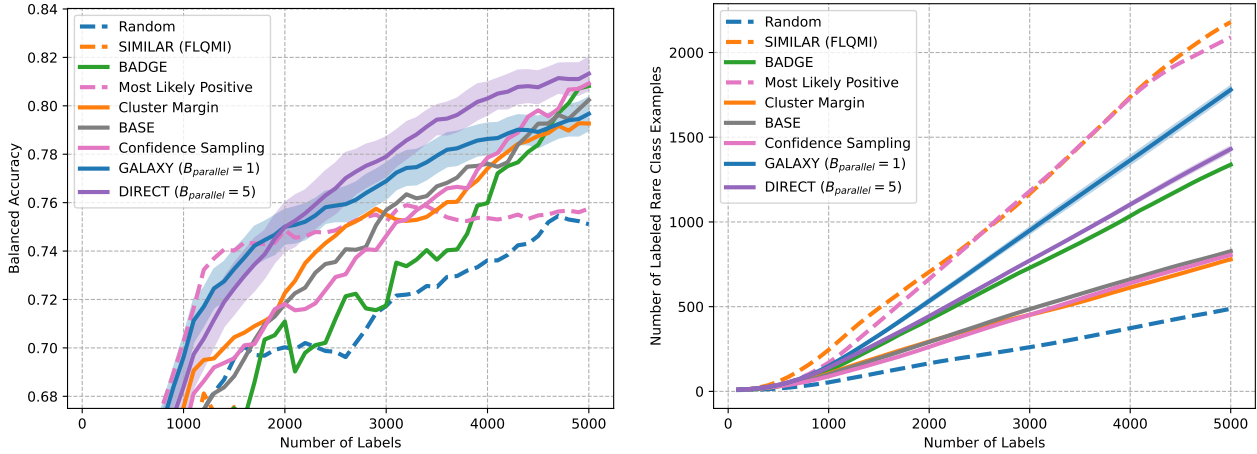
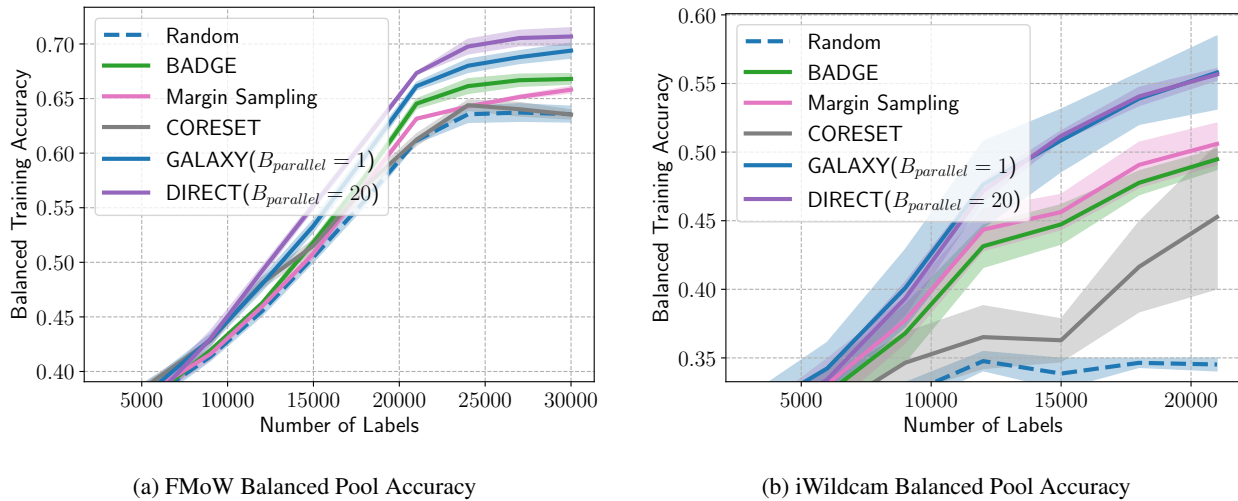


Figure 13: PathMNIST, two classes.



(a) FMoW Balanced Pool Accuracy

(b) iWildcam Balanced Pool Accuracy

Figure 14: LabelBench results in the noiseless setting.

B.2. Label Noise Results under Imbalance

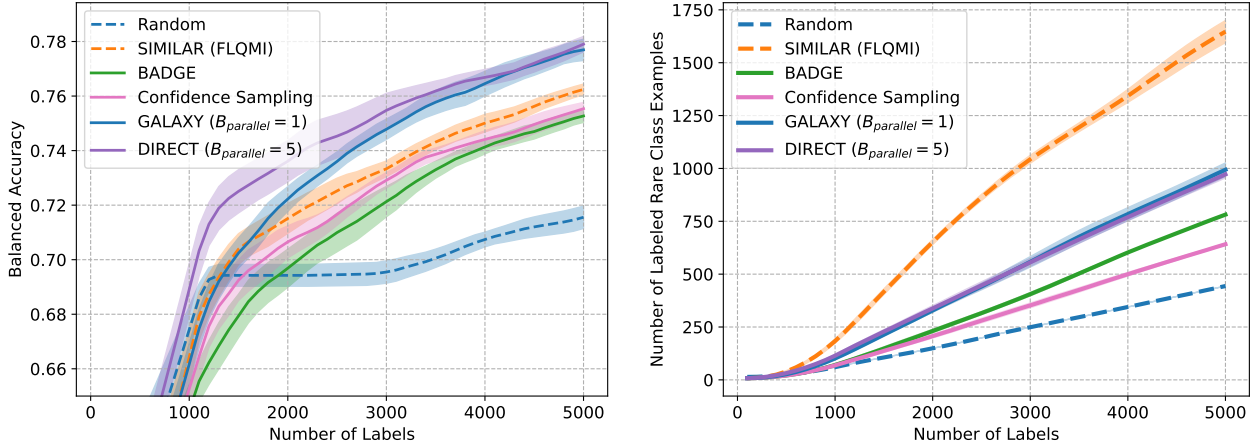


Figure 15: Imbalanced CIFAR-10, two classes, 10% label noise.

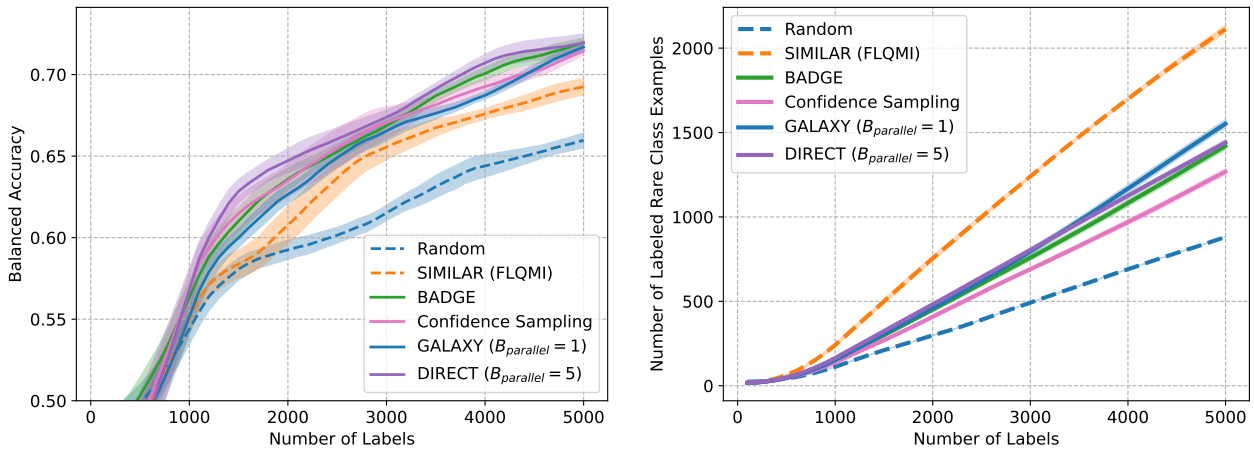


Figure 16: Imbalanced CIFAR-10, three classes, 10% label noise.

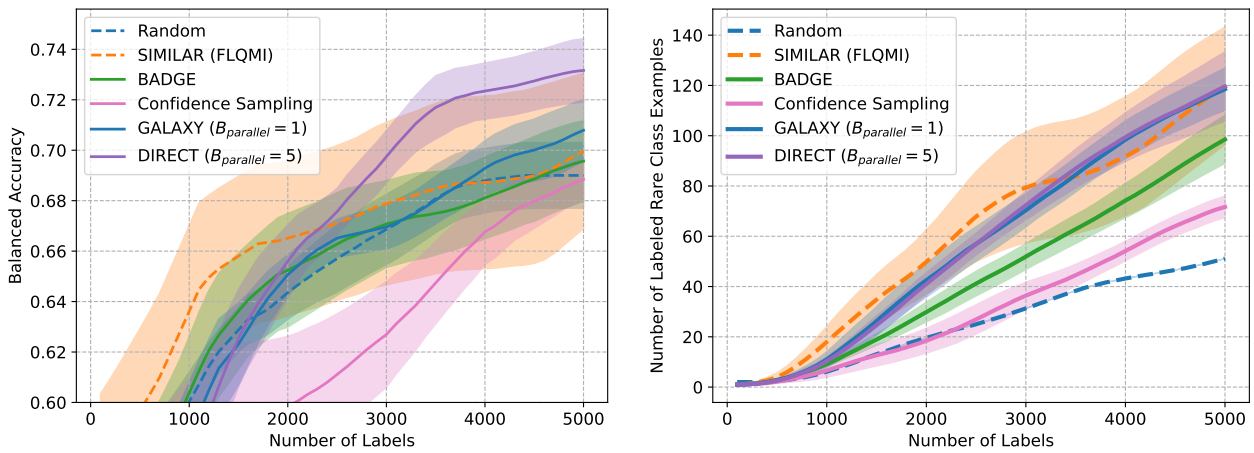


Figure 17: Imbalanced CIFAR-100, two classes, 10% label noise.

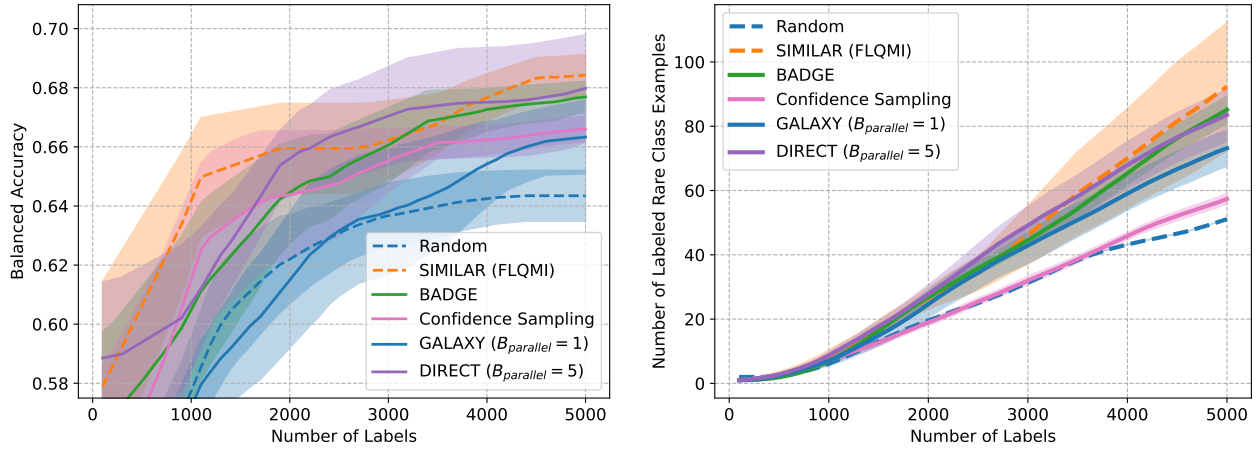


Figure 18: Imbalanced CIFAR-100, two classes, 15% label noise.

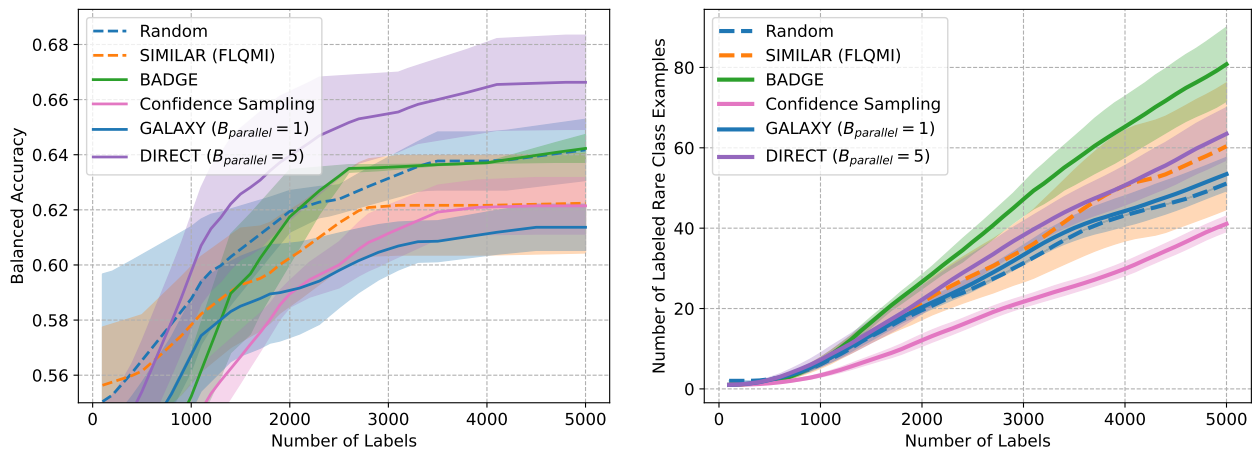


Figure 19: Imbalanced CIFAR-100, two classes, 20% label noise.

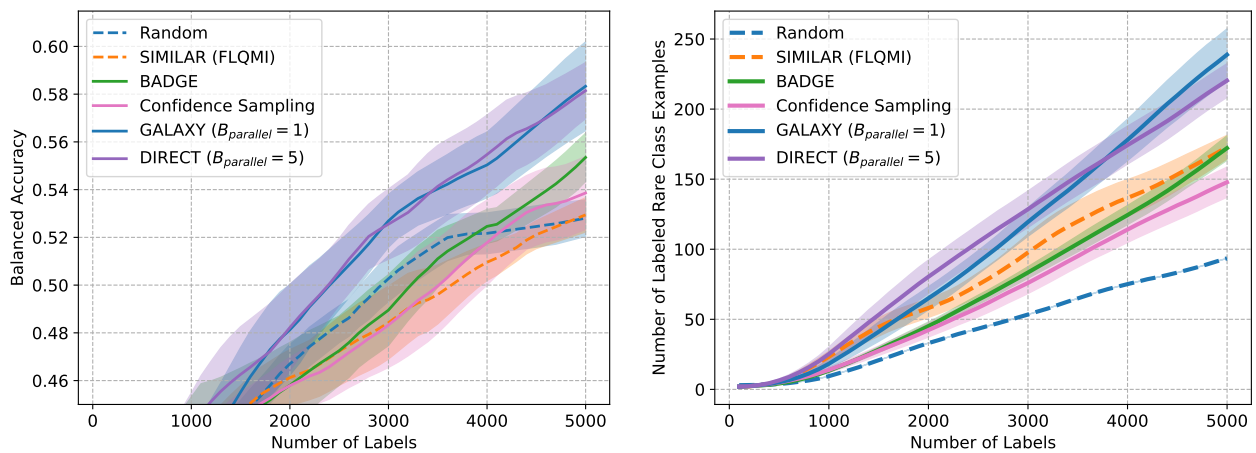


Figure 20: Imbalanced CIFAR-100, three classes, 10% label noise.

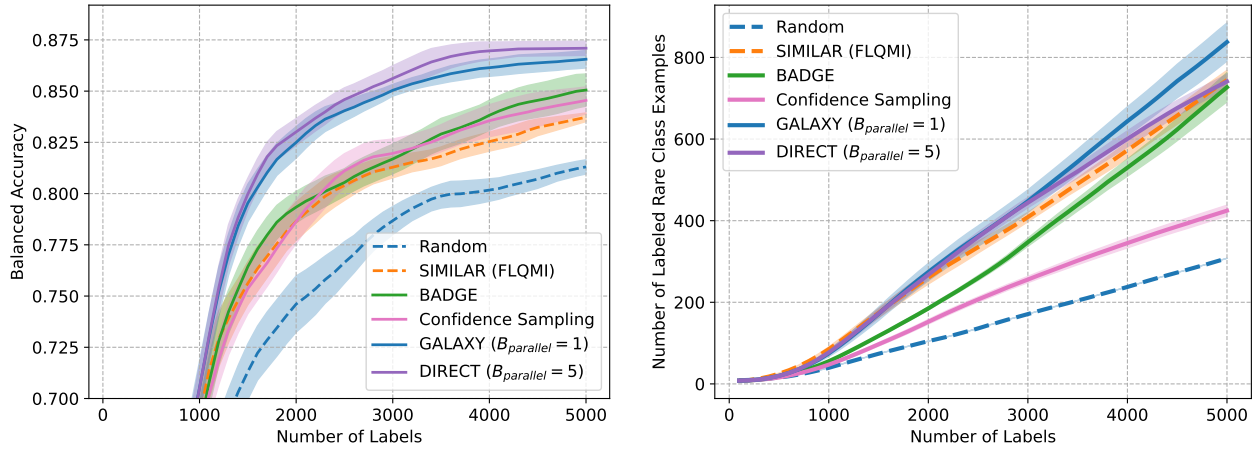


Figure 21: Imbalanced SVHN, two classes, 10% label noise.

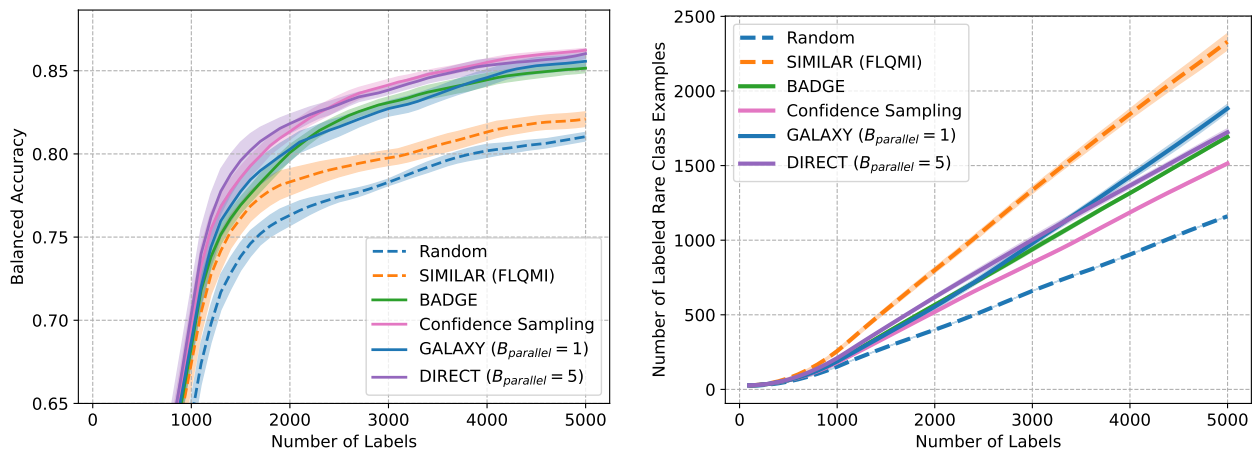
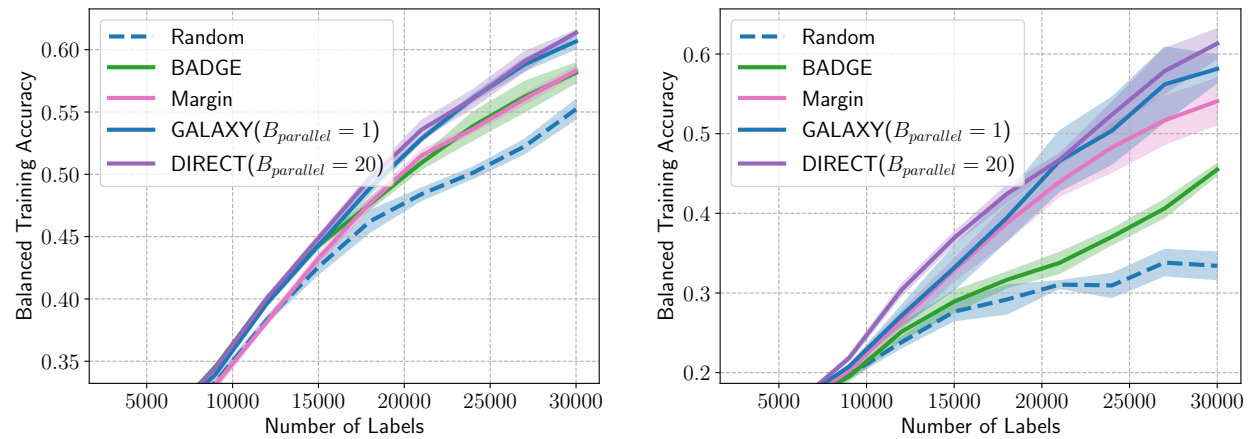


Figure 22: Imbalanced SVHN, three classes, 10% label noise.



(a) FMoW Balanced Pool Accuracy

(b) iWildcam Balanced Pool Accuracy

Figure 23: LabelBench results in the 10% label noise setting.